吡啶锰配合物诱导肿瘤细胞死亡的作用及对线粒体功能的影响

赵凯迪[1] 高 静[1]* 李 香[1] 李 瓒[2] 陈秋云[2]

([1]江苏大学药学院, 镇江 212013; [2]江苏大学化学化工学院, 镇江 212013)

摘要 研究新合成的小分子吡啶锰配合物Adpa-Mn(III)([(Adpa)Mn(μ_2-O)$_2$Mn(Adpa)]PF_6·8H_2O (Adpa=bis(2-pyridylmethyl)amino-2-propionic acid))的抗肿瘤作用, 初步探索其抗肿瘤的机制。MTT分析Adpa-Mn(III)对细胞活性的影响; 活细胞工作站观察GFP荧光标记组蛋白HeLa细胞的细胞核形态, MDC染色以及GFP-LC3质粒转染, 探讨细胞死亡的方式; JC-1染色检测线粒体膜电位; Fluo-3-AM和DCFH-DA荧光探针分别检测细胞中Ca^{2+}和ROS的含量。结果发现, Adpa-Mn(III)剂量依赖性地抑制细胞活性; 给药后细胞核出现固缩、片段化; 自噬小泡增多, GFP-LC3荧光强度增强; 线粒体膜电位下降; 细胞内Ca^{2+}发生超载, ROS含量升高。由此, Adpa-Mn(III)可抑制肿瘤细胞活性, 其机制与引起线粒体膜电位下降、增加ROS生成及诱导细胞的死亡有关, 同时胞内Ca^{2+}超载也参与了该作用。这些数据显示, Adpa-Mn(III)具有成为抗肿瘤先导金属配合物的潜在可能性。

关键词 线粒体; 自噬; 凋亡; ROS; Ca^{2+}

继王晓东等[1]发现细胞内的线粒体可释放细胞色素C, 诱导细胞凋亡之后, 线粒体已被称为“细胞生死的马达”。通过干扰线粒体的功能, 使线粒体外膜通透性发生改变, 可以诱导启动死亡程序, 包括细胞的凋亡和自噬[2-3]。目前, 线粒体已经成为筛选新型抗肿瘤药物的重要靶位之一[4-5]。

锰是人体必需的金属离子之一, 是多种酶的辅酶[6]。锰可以特异性的蓄积在线粒体内, 与钙离子竞争, 影响细胞内钙稳态[7-8]; 锰离子通过氧化还原发生二价和三价转换, 可产生自由基导致氧化损伤[9]。吡啶环有增强药物与生物大分子结合的能力, 同时吡啶类化合物也有一定的抗肿瘤作用[10-11]。本文研究的配体Adpa为二吡啶甲基胺类化合物, 本实验室已有的研究表明, Adpa可用于与多种金属离子形成具有较好抗肿瘤活性的配合物[12-15], 但是这些配合物与DNA作用较强, 具有潜在的较高的毒副作用, 而Adpa与锰形成的配合物与DNA的相互作用则比较弱。另外, 肿瘤细胞对带有吡啶、氨基等碱性基团的化合物识别能力大于正常细胞[16]。所以, 新的配合物可能通过吡啶基团提高对肿瘤组织的识别能力, 并且保留锰离子的特性, 对线粒体具有一定的靶向性, 破坏线粒体功能, 干扰肿瘤细胞能量代谢, 从而诱导肿瘤细胞死亡。本实验对新合成的[(Adpa)Mn(μ_2-O)$_2$Mn(Adpa)]PF_6·8H_2O(母核结构见图1, 引自参考文献[17])诱导肿瘤细胞死亡的作用以及机制进行了初步研究, 为此类药物的研发打下基础。

1 材料与方法

1.1 药品

[(Adpa)Mn(μ_2-O)$_2$Mn(Adpa)]PF_6·8H_2O由江苏大学化学化工学院陈秋云教授研究组合成。贮存液(100 mmol/L)用二甲亚砜(DMSO)配制。应用液以含10%血清培养基稀释。

1.2 细胞株及培养

人肝癌细胞(HepG2)、人宫颈癌细胞(HeLa)、人非小细胞肺癌细胞(A549)、人脑胶质瘤细胞株(U251)和正常永生化肝细胞(WRL-68)购于中科院上海细胞库; 组蛋白(H_2B)稳定转染HeLa细胞株(H_2B-GFP labeled HeLa)由南京大学李朝军教授惠赠。用含10%小牛血清或胎牛血清(杭州四季青生物工程有限公司)的RPMI1640/MEM/DMEM(Gibco)培养液在37 ºC、5% CO_2及饱和湿度的培养箱中培养。

收稿日期: 2012-02-28 接受日期: 2012-03-30

国家自然科学基金(No.20971059/B0104)、江苏省自然科学基金(No.BK2008244)和镇江市社会发展项目(No.SH2008072) 资助项目

*通讯作者。Tel/Fax: 0511-88791552, E-mail: jinggao@ujs.edu.cn

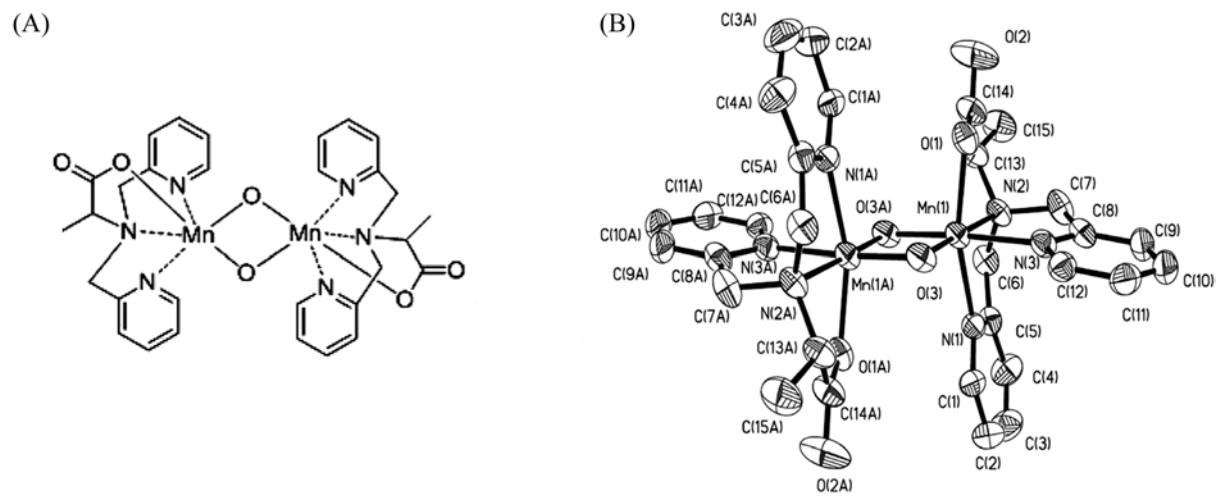

A: 化学结构; B: 晶体结构。

A: chemical constitution; B: crystal structures.

图1 $[(Adpa)Mn(\mu_2\text{-}O)_2Mn(Adpa)]^+$的结构[17]

Fig.1 The structure of $[(Adpa)Mn(\mu_2\text{-}O)_2Mn(Adpa)]^+$[17]

1.3 主要仪器及试剂

HealForce CO_2孵箱; TS100 Nikon倒置相差显微镜; Spectra Max 190酶标仪; Spectra MaxGemini荧光酶标仪; Nikon eclipse Ti-E活细胞荧光工作站; Hoechst 33342荧光染料(南通碧云天生物技术有限公司); 自噬荧光染料MDC(Sigma公司); JC-1荧光染料(Molecular Probes公司); DCFH-DA荧光探针(南通碧云天生物技术有限公司); Fluo-3-AM(Sigma公司)。

1.4 MTT法检测细胞活性

取对数生长期细胞, 消化、计数, 以 4×10^4/mL的密度接种于96孔培养板中, 每孔100 μL。培养24 h后以不同浓度化合物处理肿瘤细胞。药物作用48 h后, 去上清, 每孔加入100 μL MTT(1 mg/mL), 继续培养4 h, 弃上清, 每孔加入100 μL DMSO, 1 h后用酶标仪在570 nm处测定吸光度值。抑制率(%) = (1–给药组吸光度值/对照组吸光度值)×100%。

1.5 活细胞工作站观察细胞核形态变化

取对数生长期H_2B-GFP labeled HeLa细胞, 以4×10^4/mL的密度接种于24孔培养板中, 每孔500 μL。培养24 h后给药, 在Nikon eclipse Ti-E活细胞荧光工作站下观察。

1.6 MDC染色检测, LC3质粒转染检测细胞自噬

作为自噬的特征, 细胞内酸性小泡的形成使用MDC染色进行检测。细胞经药物处理后吸掉培养基, 加入50 mmol/L MDC 37 ºC孵育15 min, 然后PBS洗两次, 在荧光显微镜下观察。

细胞采用脂质体2000质粒转染试剂盒进行质粒GFP-LC3转染。4 h后弃去上清, 加入药物进行处理, 在荧光显微镜下观察。

1.7 JC-1染色检测线粒体膜电位

线粒体膜电位可由荧光染料JC-1来反映。JC-1的特性是当膜电位小于100 mV时会以单体的形式存在于线粒体内膜, 在490 nm激发光下会形成绿色荧光(发射光525 nm); 而当膜电位升高时, JC-1会聚集在线粒体内膜形成橙色荧光(发射光590 nm); 反之, 当膜电位下降时, JC-1又会以绿色荧光的单体形式存在。药物处理细胞后吸掉培养基, 加入5 mg/mL JC-1 37 ºC孵育30 min, 然后PBS洗两次, 在荧光显微镜下观察或使用荧光酶标仪检测荧光强度。

1.8 DCFH-DA荧光探针检测细胞内ROS水平

细胞内ROS水平使用DCFH-DA荧光探针检测。药物处理细胞后吸掉培养基, 加入无血清培养基稀释的DCFH-DA溶液, 使其终浓度为10 μmol/L, 37 ºC孵育30 min, 然后PBS洗两次, 在荧光显微镜下观察或使用荧光酶标仪检测荧光强度。

1.9 Fluo-3-AM荧光探针检测细胞内Ca^{2+}含量

细胞内Ca^{2+}含量使用Fluo-3-AM荧光探针来检测。药物处理细胞后吸掉培养基, 加入3 μg/mL Fluo-3-AM 37 ºC孵育30 min, 然后PBS洗两次, 在荧光显微镜下观察或使用荧光酶标仪检测荧光强度。

1.10 统计方法

采用SAS统计软件, ANOVA方差分析, 数据以平

均数±标准差(means±SD)表示。各实验至少重复3次。

2 结果

2.1 Adpa-Mn(III)对细胞活性的影响

结果显示, Adpa-Mn(III)有效地抑制HepG2细胞、HeLa细胞、A549细胞以及U251细胞增殖(图2), 且IC_{50}值都在10 μmol/L左右(表1)。倒置相差显微镜下观察可见, 作用48 h后, 细胞形态发生明显改变, 细胞皱缩、变圆、数量减少(图3)。说明Adpa-Mn(III)对肿瘤细胞具有抑制增殖、诱导细胞损伤的作用。比较Adpa-Mn(III)对肿瘤细胞(HepG2)和正常细胞(WRL-68)的作用可以发现, Adpa-Mn(III)对正常细胞的抑制作用明显小于对肿瘤细胞的抑制作用(图4)。同时, Adpa-Mn(III)可时间剂量依赖性的抑制U251细胞增殖(图5)。

2.2 Adpa-Mn(III)对细胞核形态的影响

由图6A可以看出, 随着药物作用时间的延长, GFP标记的Hela细胞的细胞核出现固缩、片段化等典型的凋亡特征(箭头所指处)。对具有凋亡特征的细胞核进行统计, 药物作用24 h后其占总细胞数的20%左右(图6B)。说明Adpa-Mn(III)可能诱导细胞发生了凋亡, 但是凋亡率比较低。

2.3 Adpa-Mn(III)诱导细胞的死亡方式

由图7可以看出, U251细胞经MDC染色, 药物作用24 h后细胞荧光强度明显强于对照组。LC3蛋白在自噬过程中起着关键的作用, 使用GFP-LC3质粒转染U251细胞, 给药24 h后, 荧光发生聚集, 且荧光强度明显增加(图8), 说明LC3蛋白表达增加, Adpa-Mn(III)诱导细胞发生了自噬。

2.4 Adpa-Mn(III)对细胞线粒体膜电位的影响

将不同浓度的Adpa-Mn(III)作用于U251细胞,

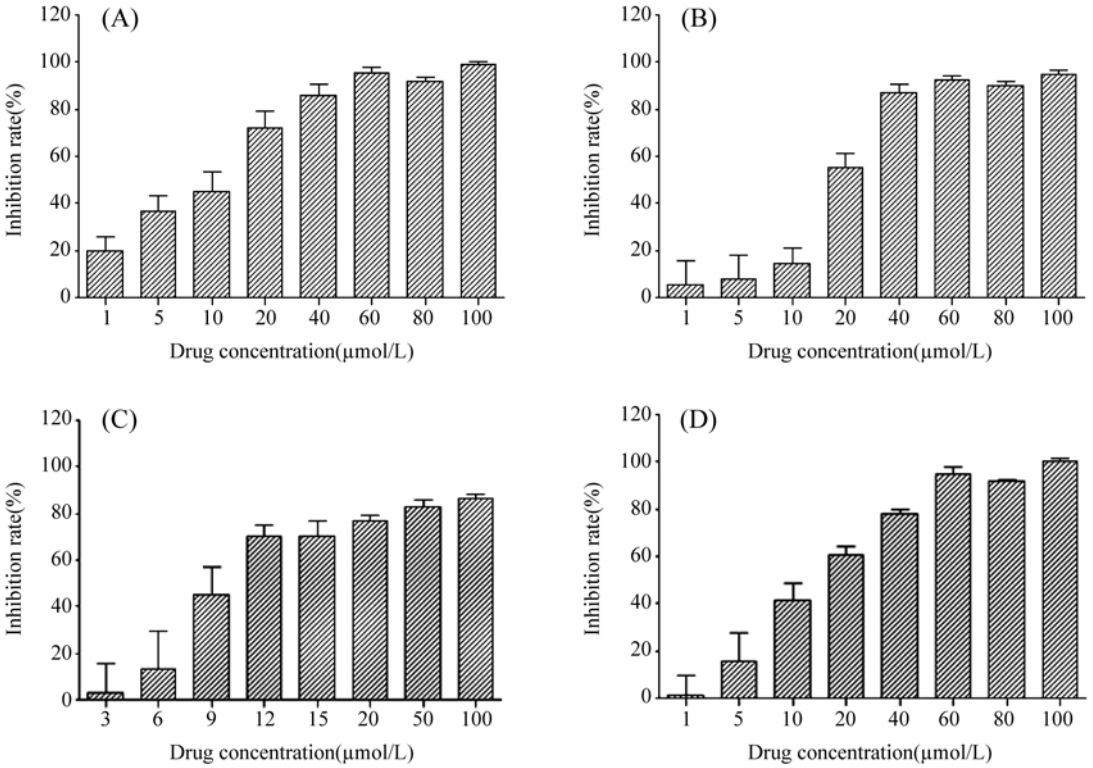

A: U 251; B: HeLa; C: A549; D: HepG2. means±SD, *n*=5.

图2 Adpa-Mn(III)抑制不同肿瘤细胞的增殖

Fig.2 Proliferation inhibition of Adpa-Mn(III) on different cancer cell lines

表1 Adpa-Mn(III)作用48 h抑制不同肿瘤细胞株的IC_{50}值

Table 1 IC_{50} of Adpa-Mn(III) on different tumor cell lines for 48 h

细胞株 Cell line	IC_{50}(μmol/L)
HeLa	15.2
U251	10.2
A549	14.2
HepG2	17.5

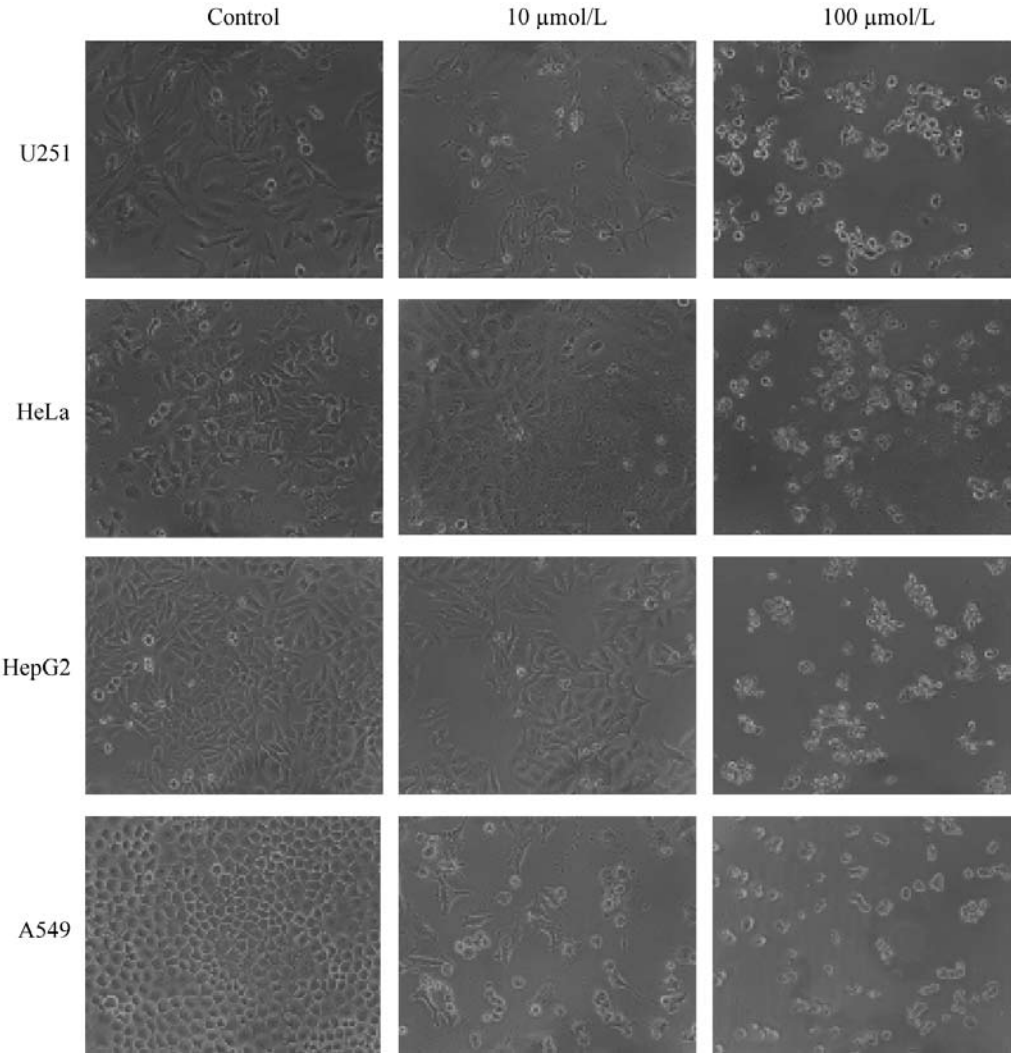

图3 Adpa-Mn(III)抑制各肿瘤细胞增殖的形态学观察(100×)

Fig.3 The morphological changes were induced by Adpa-Mn(III) in cancer cells for 48 h(100×)

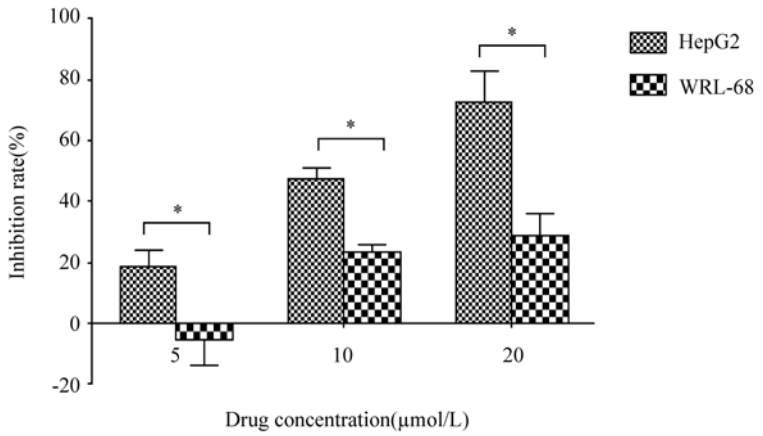

使用不同浓度Adpa-Mn(Ⅲ)处理HepG2细胞和WRL-68细胞, 48 h后MTT法检测细胞活性。Means±SD, n=5, *P<0.05.

HepG2 cells and WRL-68 cells were treated by different concentration of Adpa-Mn(Ⅲ) for 48 h. Cell proliferation was determined by MTT assay. Means±SD, n=5, *P<0.05.

图4 Adpa-Mn(III)对HepG2细胞和WRL-68细胞的抑制作用

Fig.4 Proliferation inhibition of Adpa-Mn(III) on HepG2 cells and WRL-68 cells

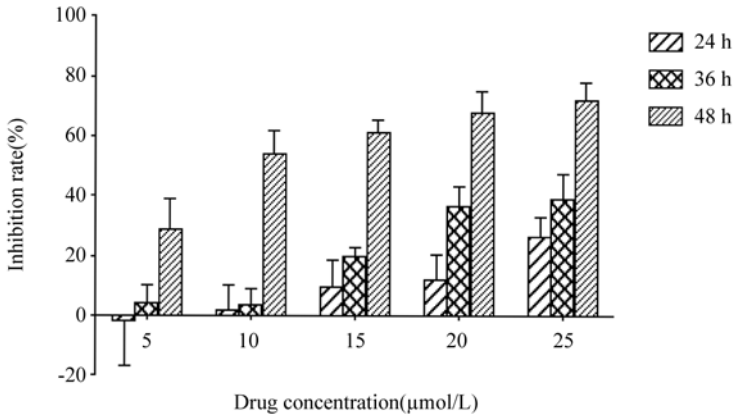

图5　Adpa-Mn(III)时间剂量依赖性抑制U251细胞增殖

Fig.5　Dose- and time-dependent effect of Adpa-Mn(III) on U251 proliferation

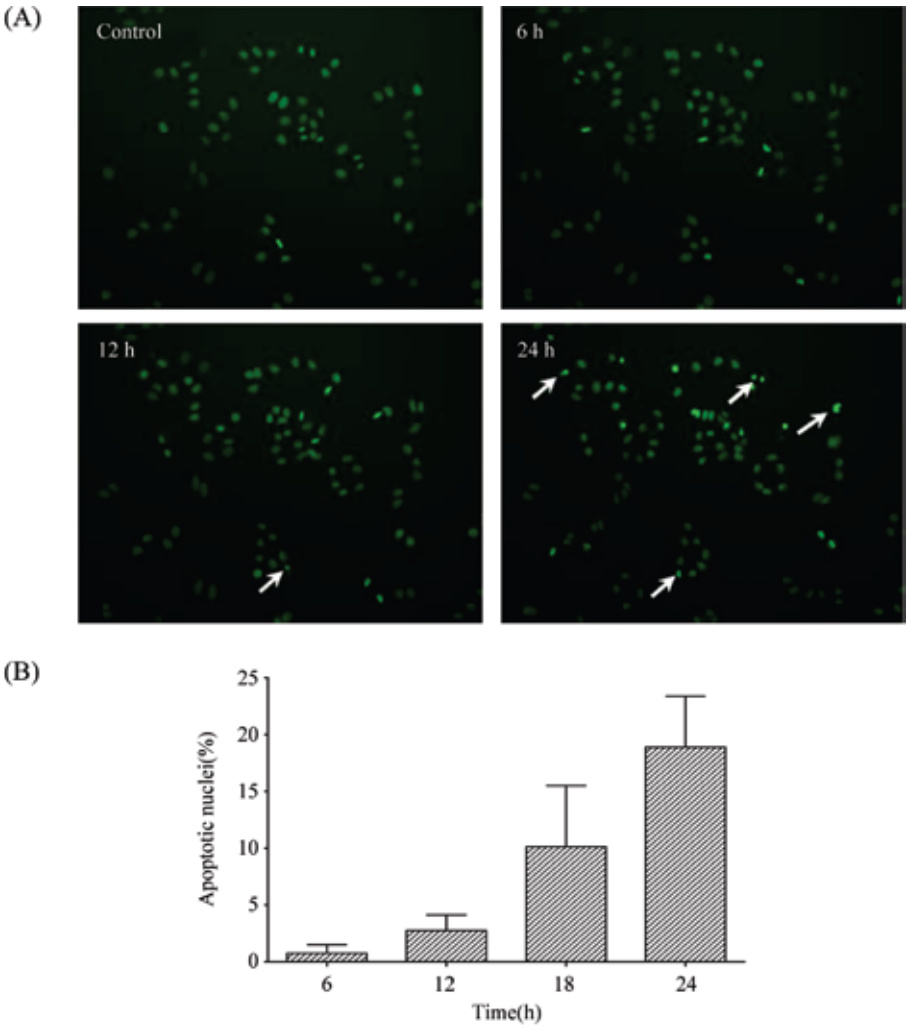

A: 细胞使用15 μmol/L Adpa-Mn(III)处理后在活细胞工作站下观察细胞及细胞核的形态学变化, 观察24 h; B: 每个时间点随机选取5个视野, 对凋亡样细胞核进行计数, 并计算占视野总细胞数的百分比。

A: cells were exposed to 15 μmol/L of Adpa-Mn(III), then observe the morphological changes of the cells and nuclei under the LCS. This process lasted for over 24 hours. B: apoptotic nuclei were counted from 5 eyesights each time point and the percent was calculated.

图6　活细胞工作站观察Adpa-Mn(III)引起GFP核标记的Hela细胞凋亡(200×)

Fig.6　Adpa-Mn(III) induced apoptosis in H_2B-labled HeLa cells by using a live cell system(LCS)(200×)

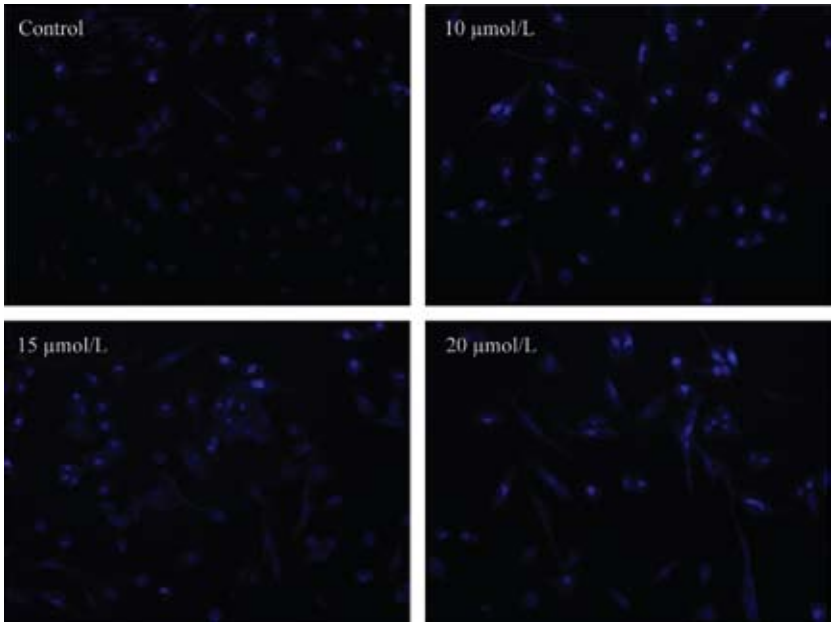

图7 Adpa-Mn(III)处理U251细胞后MDC染色增强(200×)

Fig.7 Adpa-Mn(III) treatment enhanced MDC staining in U251 cells(200×)

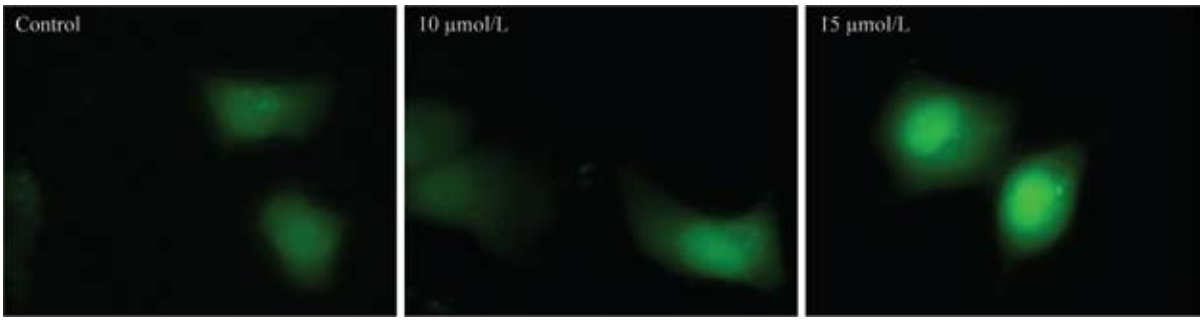

图8 Adpa-Mn(III)处理U251细胞后GFP-LC3荧光强度增强(400×)

Fig.8 Adpa-Mn(III) treatment enhanced the fluorescence of GFP-LC3 in A549 cells(400×)

用JC-1染色通过荧光显微镜观察并测荧光度。如图9A所示, Adpa-Mn(III)处理的U251细胞红光减弱、绿光增强, 说明U251细胞的线粒体膜电位降低。随着Adpa-Mn(III)的浓度增加, U251细胞线粒体膜电位降低的程度也随之增加。如图9B所示, 测定给药后的红、绿荧光强度比值, 与对照组相比, 随着Adpa-Mn(III)浓度的增加, 红、绿荧光强度比值明显下降。从而进一步说明, Adpa-Mn(III)通过降低肿瘤细胞线粒体膜电位诱导细胞死亡。

2.5 Adpa-Mn(III)对细胞内ROS的影响

ROS在正常的细胞代谢中必不可少, 但是过量的ROS会导致氧化损伤, 进而导致细胞的死亡。故采用DCFH-DA染色检测U251细胞内ROS的含量。分析图10A中的荧光照片, 正常组中存在一定强度的绿色荧光, 这是维持细胞正常功能所必需的, 而经过10 μmol/L的Adpa-Mn(III)处理以后, 绿色荧光剧烈增强。对荧光信号进行定量分析, 如图10B所示: 以10 μmol/L的Adpa-Mn(III)作用U251细胞不同时间, 与对照组相比, 处理6 h后, 10^4个细胞荧光强度增加到1.5倍, 说明细胞内活性氧显著升高。随着化合物作用时间的延长, 细胞内ROS的含量继续增加。

2.6 Adpa-Mn(III)对细胞内Ca^{2+}的影响

钙离子是线粒体功能的一个关键调节因子, 在对于细胞器和刺激ATP的合成中起着重要的作用。用Fluo-3-染色, 荧光显微镜观察U251细胞内钙离子浓度的变化, 结果如图11所示, 5 μmol/L Adpa-Mn(III)作用24 h荧光强度略有增强, 与对照组相比, 平均荧光强度升高, Ca^{2+}的荧光强度随着Adpa-

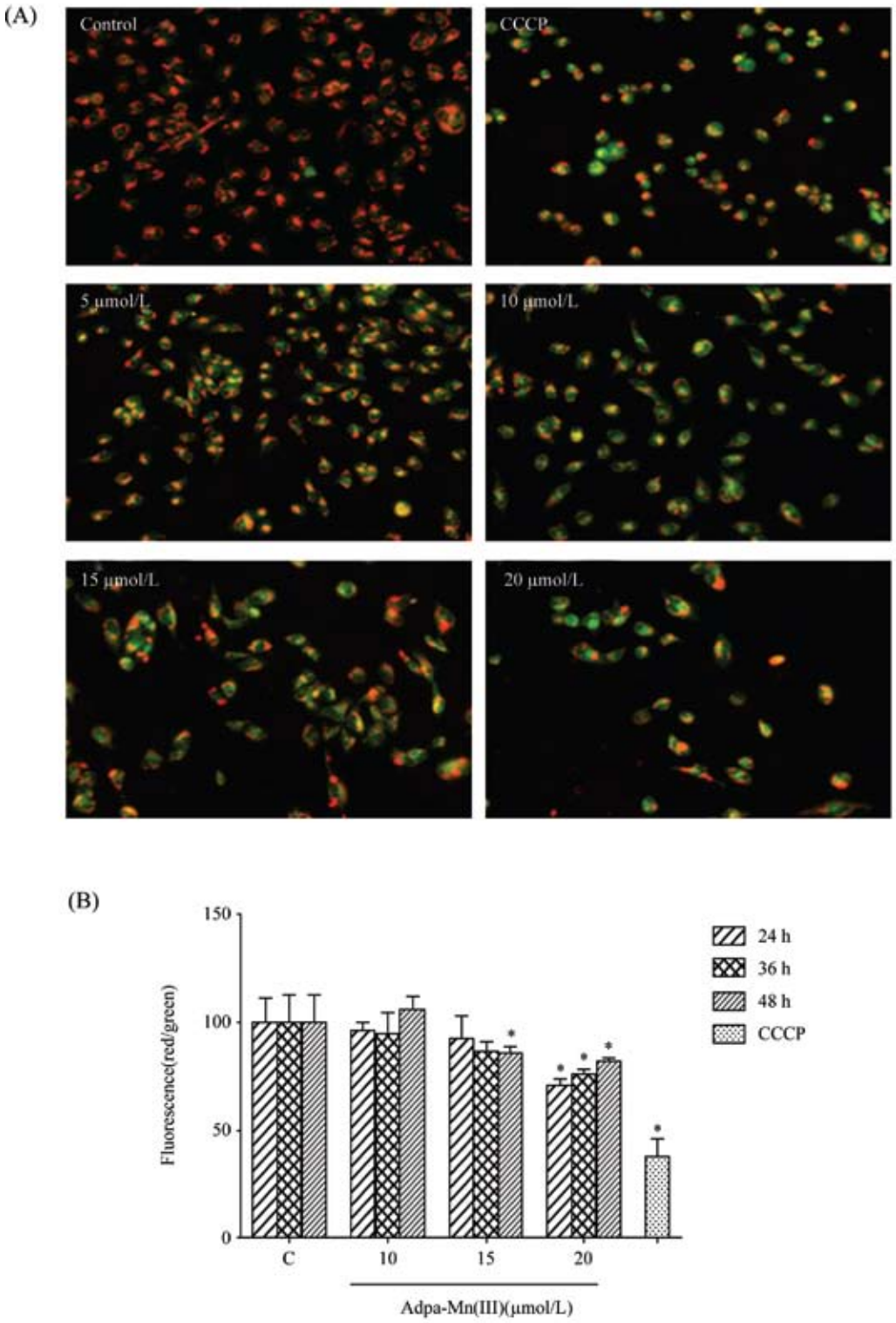

A: 细胞使用不同浓度的Adpa-Mn(III)处理48 h, 线粒体使用JC-1染色, 在Nikon荧光显微镜下观察(200×); B: Adpa-Mn(III)时间剂量依赖性的降低U251细胞中JC-1的红/绿荧光比值, means±SD, n=5, 与对照组相比, *P<0.05。

A: cells were exposed to Adpa-Mn(III) with different concerntration for 48 h. The change of mitochondrial stained with JC-1 were visualized by using Nikon Fluorescence microscope(200×); B: dose and time-dependent decrease of the red/green fluorescence ratio of JC-1 by treatment with Adpa-Mn(III) in U251 cells, means±SD, n=5,*P<0.05 vs control.

图9　Adpa-Mn(III)诱导U251线粒体膜电位下降

Fig.9　Adpa-Mn(III)-induced mitochondrial membrane potential collapse in U251 cells

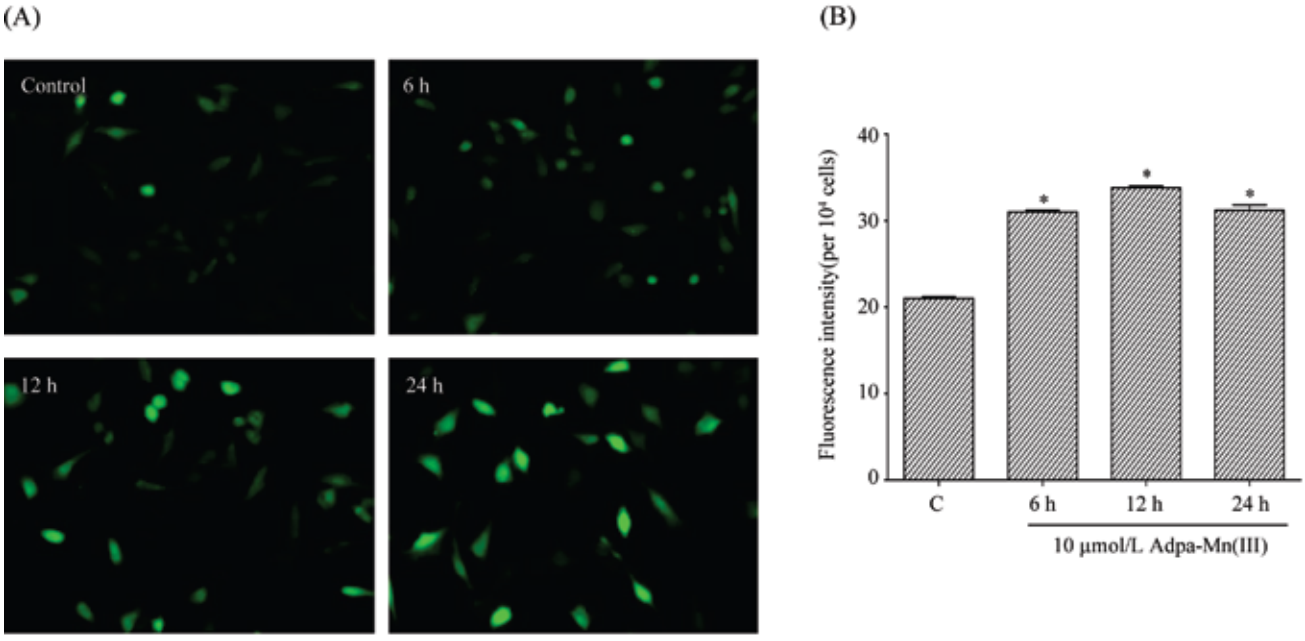

A: 细胞使用10 μmol/L Adpa-Mn(III)处理不同时间后拍摄荧光照片(200×); B: 细胞使用10 μmol/L Adpa-Mn(III)处理不同时间后使用荧光酶标仪检测荧光强度, means±SD, n=3, 与对照组相比, *P<0.05。

A: cells were treated by 10 μmol/L Adpa-Mn(III) for different time, fluorescence photo were taken(200×) B: cells were treated by 10 μmol/L Adpa-Mn(III) for different hours, fluorescence intensity were detected by spectrophotofluorimeter, means±SD, n=3, *P<0.05 vs control.

图10 Adpa-Mn(III)诱导U251细胞内ROS的产生

Fig.10 Adpa-Mn(III) trigger ROS generation in U251 cells

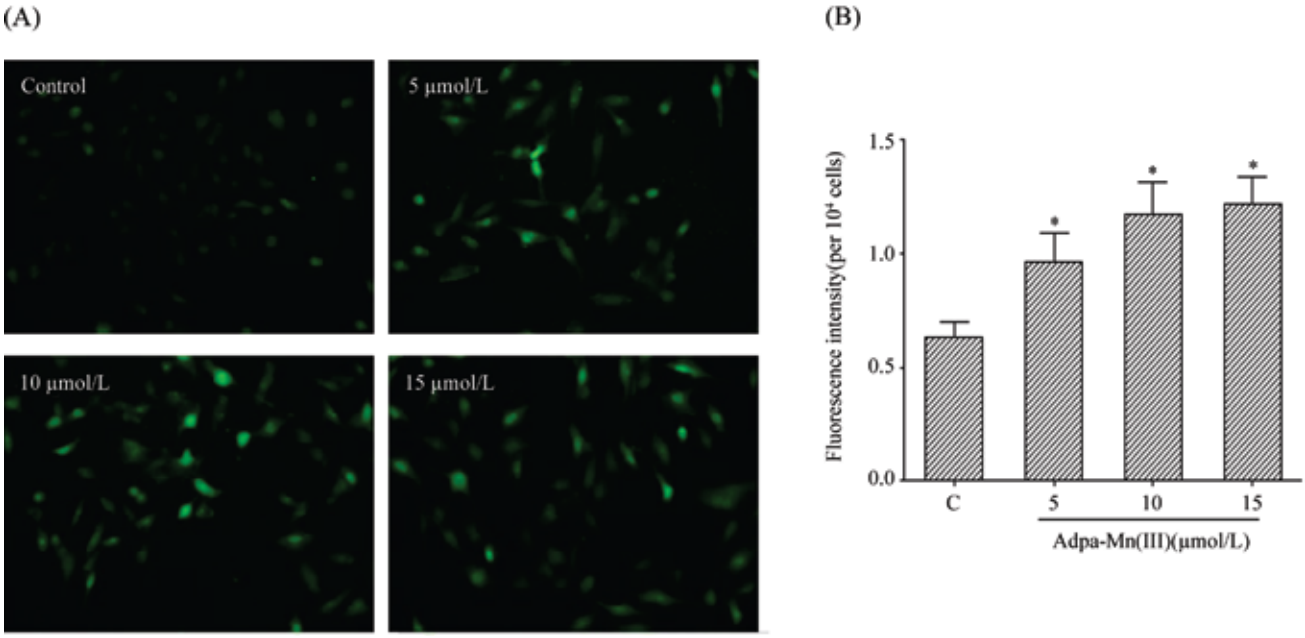

A: Adpa-Mn(III)处理细胞24 h后拍摄荧光照片(200×); B: 使用荧光酶标仪检测荧光强度, means±SD, n=6, 与对照组相比, *P<0.05。

A: cells were treated by Adpa-Mn(III) for 24 h, fluorescence photos were taken(200×); B: fluorescence intensity were detected, means±SD, n=6, *P<0.05 vs control.

图11 Adpa-Mn(III)引起U251细胞内Ca^{2+}超载

Fig.11 Intracellular Ca^{2+} overload was induced by Adpa-Mn(III)

Mn(III)作用浓度的升高而增强, 说明Adpa-Mn(III)可诱导胞内钙离子超载。

3 讨论

随着顺铂在抗肿瘤方面的应用, 引起无机药物化学研究的热潮。早期无机抗肿瘤药物多是围绕着二价铂类配合物进行研究, 虽然可以影响线粒体的功能, 但这些化合物多数是以DNA为靶点, 干扰DNA的功能, 且对肿瘤细胞识别能力弱, 毒性较大。二吡啶甲基胺以及它的衍生物被认为是一种优良的多齿配体, 由于其吡啶上的氮原子和烷基胺上的氮原子能够与多种金属配位而形成稳定的配合物, 并且这些配合物具有生物、金属有机以及催化活性, 而被广泛的应用于配位化学领域[18]。本实验中配体Adpa与锰形成十分稳定的配合物, 利用肿瘤细胞对带有吡啶等碱性基团化合物识别能力大于正常细胞的特点, 以及锰的线粒体靶向性, 提高药物对肿瘤细胞和线粒体的识别作用。本实验观察到, Adpa-Mn(III)可以抑制多种不同组织来源的肿瘤细胞增殖, 并且对正常细胞的抑制作用较弱, 表现出良好的抗肿瘤活性。

目前, 很多临床上使用的化疗药物都能通过诱导肿瘤发生凋亡(I型程序性死亡)的机理来治疗肿瘤, 然而由于肿瘤细胞中凋亡通路往往存在缺陷, 所以极易产生耐药性[19-20]。而自噬(Ⅱ型程序性死亡)可以作为一个可能的抗肿瘤机制有效地抑制凋亡耐受的肿瘤细胞。

本实验观察到, GFP核标记的Hela细胞在Adpa-Mn(III)作用下, 细胞出现皱缩、出泡的现象, 细胞核出现固缩、片段化等凋亡样变化, 但是发生凋亡样变化的细胞核比例并不高。而MDC染料可被细胞吸收并选择性地聚集于自噬小泡(autophagic vacuoles)中, 在荧光显微镜的观察下呈现出点状结构, 这就使得自噬的活化可被形象地检测到。实验中观察到, 给药组细胞荧光强度明显强于对照组。同时, GFP-LC3荧光强度显著增强, 说明LC3蛋白的表达量增加。提示Adpa-Mn(III)可以诱导肿瘤细胞发生凋亡和自噬而导致细胞死亡, 而且自噬很可能在其中起着更重要的作用。

在凋亡和自噬的过程中, 线粒体都起着直接或间接的调节作用[21-22]。线粒体外膜(outer mitochondrial membrane, OMM)的透化作用, 即通透性增加, 表现为线粒体跨膜电位Δψ的下降, 导致一些促凋亡蛋白(特别是细胞色素C)从线粒体膜间隙释放至胞浆, 继而触发凋亡。线粒体膜电位Δψ的降低是细胞发生凋亡的标志事件[23]。一旦线粒体跨膜电位Δψ崩溃, 则细胞凋亡不可逆转。最新的研究发现, 线粒体上还存在参与自噬体形成的调控因子(受体: Atg32), 线粒体功能改变可启动自噬[24-26]。自噬、凋亡和坏死可能都是线粒体对胞内信号的统一调控下的不同结果[27]。而ROS[28-29]和Ca^{2+}[30-32]在这些过程中起着十分重要的作用。

本研究显示, Adpa-Mn(III)时间剂量依赖性的降低线粒体膜电位, 在15 μmol/L的浓度作用48 h后线粒体膜电位发生明显下降(图8)。在此之前, 15 μmol/L的Adpa-Mn(III)处理U251细胞24 h后, 细胞内Ca^{2+}就已发生超载(图10)。而且, 10 μmol/L的Adpa-Mn(III)处理U251细胞6 h后, 细胞内的ROS水平就明显升高(图9)。说明Adpa-Mn(III)可能通过破坏线粒体功能, 增加ROS的产生, 诱导细胞内Ca^{2+}超载, 继而导致线粒体外膜通透性的改变, 线粒体膜电位下降, 启动细胞死亡进程, 导致细胞发生凋亡和自噬, 从而抑制肿瘤细胞的增殖。

综上所述, Adpa-Mn(III)通过线粒体介导的通路诱导肿瘤细胞发生凋亡和自噬, 抑制肿瘤细胞的增殖。此外, 肿瘤细胞靶向性的探讨以及在体抗肿瘤活性的检测仍需进一步研究, 以证实Adpa-Mn(III)作为抗肿瘤先导化合物的有效性。

参考文献 (References)

1 Liu X, Kim CN, Yang J, Jemmerson R, Wang X. Induction of apoptotic program in cell-free extracts: Requirement for dATP and cytochrome c. Cell 1996; 86(1): 147-57.

2 Jana S, Paliwal J. Apoptosis: Potential therapeutic targets for new drug discovery. Curr Med Chem 2007; 14(22): 2369-79.

3 Scherz-Shouval R, Elazar Z. ROS, mitochondria and the regulation of autophagy. Trends Cell Biol 2007; 17(9): 422-7.

4 Wenner CE. Targeting mitochondria as a therapeutic target in cancer. J Cell Physiol 2012; 227(2): 450-6.

5 Gogvadze V, Orrenius S, Zhivotovsky B. Mitochondria as targets for cancer chemotherapy. Semin Cancer Biol 2009; 19(1): 57-66.

6 Takeda Y, Avila H. Structure and gene expression of the *E. coli* Mn-superoxide dismutase gene. Nucleic Acids Res 1986; 14(11): 4577-89.

7 Tialkens RB, Zoran MJ, Mohl B, Barhoumi R. Manganese suppresses ATP-dependent intercellular calcium waves in astrocyte

networks through alteration of mitochondrial and endoplasmic reticulum calcium dynamics. Brain Res 2006; 1113(1): 210-9.

8 Gunter TE, Gavin CE, Aschner M, Gunter KK. Speciation of manganese in cells and mitochondria: A search for the proximal cause of manganese neurotoxicity. Neurotoxicology 2006; 27(5): 765-76.

9 Gunter TE, Gavin CE, Gunter KK. The case for manganese interaction with mitochondria. Neurotoxicology 2009; 30(4): 727-9.

10 Regino CA, Torti SV, Ma R, Yap GP, Kreisel KA, Torti FM*, et al.* N-picolyl derivatives of Kemp's triamine as potential antitumor agents: A preliminary investigation. J Med Chem 2005; 48(25): 7993-9.

11 Chaston TB, Watts RN, Yuan J, Richardson DR. Potent antitumor activity of novel iron chelators derived from di-2-pyridylketone isonicotinoyl hydrazone involves fenton-derived free radical generation. Clin Cancer Res 2004; 10(21): 7365-74.

12 Huang J, Chen QY, Wang LY, Fu HJ, Li B. Synthesis, interaction with DNA and a ntitumor activities of Zinc(II) complexes with N-substituted Di(picolyl)amines. Chin Inorg Chem 2009; 25(6): 1077-83.

13 Guo WJ, Ye SS, Cao N, Huang J, Gao J, Chen QY. ROS-mediated autophagy was involved in cancer cell death induced by novel copper (II) complex. Exp Toxicol Pathol 2010; 62(5): 577-82.

14 Wang LY, Chen QY, Huang J, Wang K, Feng CJ, Gen ZR. Synthesis, characterization, and bioactivities of copper complexes with N-substituted Di(picolyl) amines. Transition Met Chem 2009; 34(3): 337-45.

15 Qiu-Yun C, Dong-Fang Z, Juan H, Wen-Jie G, Jing G. Synthesis, anticancer activities, interaction with DNA and mitochondria of manganese complexes. J Inorg Biochem 2010; 104(11): 1141-7.

16 Desany B, Zhang Z. Bioinformatics and cancer target discovery. Drug Discov Today 2004; 9(18): 795-802.

17 Zhou DF, Chen QY, Qi Y, Fu HJ, Li Z, Zhao KD*, et al.* Anticancer activity, attenuation on the absorption of calcium in mitochondria, and catalase activity for manganese complexes of N-Substituted Di (picolyl) amine. Inorg Chem 2011; 50(15): 6929-37.

18 Ronconi L, Sadler PJ. Using coordination chemistry to design new medicines. Coord Chem Rev 2007; 251(13): 1633-48.

19 Gong JG, Costanzo A, Yang HQ, Melino G, Kaelin WG, Levrero M*, et al.* The tyrosine kinase c-Abl regulates p73 in apoptotic response to cisplatin-induced DNA damage. Nature 1999; 399(6738): 806-9.

20 Johnstone RW, Ruefli AA, Lowe SW. Apoptosis: A link between cancer genetics and chemotherapy. Cell 2002; 108(2): 153-64.

21 Lemasters JJ, Qian T, He L, Kim JS, Elmore SP, Cascio WE*, et al.* Role of mitochondrial inner membrane permeabilization in necrotic cell death, apoptosis, and autophagy. Antioxid Redox Sig 2002; 4(5): 769-81.

22 Martinou JC, Youle RJ. Mitochondria in apoptosis: Bcl-2 family members and mitochondrial dynamics. Dev cell 2011; 21(1): 92-101.

23 Bouchier-Hayes L, Lartigue L, Newmeyer DD. Mitochondria: Pharmacological manipulation of cell death. J Clin Invest 2005; 115(10): 2640-7.

24 Okamoto K, Kondo-Okamoto N, Ohsumi Y. Mitochondria-anchored receptor Atg32 mediates degradation of mitochondria via selective autophagy. Devcell 2009; 17(1): 87-97.

25 Kanki T, Wang K, Cao Y, Baba M, Klionsky DJ. Atg32 is a mitochondrial protein that confers selectivity during mitophagy. Dev cell 2009; 17(1): 98-109.

26 Ishihara N, Mizushima N. A receptor for eating mitochondria. Dev cell 2009; 17(1): 1-2.

27 Matsunaga K, Saitoh T, Tabata K, Omori H, Satoh T, Kurotori N*, et al.* Two Beclin 1-binding proteins, Atg14L and Rubicon, reciprocally regulate autophagy at different stages. Nat Cell Biol 2009; 11(4): 385-96.

28 Scherz-Shouval R, Shvets E, Fass E, Shorer H, Gil L, Elazar Z. Reactive oxygen species are essential for autophagy and specifically regulate the activity of Atg4. EMBO J 2007; 26(7): 1749-60.

29 Huang J, Lam GY, Brumell JH. Autophagy signaling through reactive oxygen species. antioxid redox signal 2011; 14(11): 2215-31.

30 Orrenius S, Zhivotovsky B, Nicotera P. Regulation of cell death: the calcium-apoptosis link. Nat Rev Mol Cell Biol 2003; 4(7): 552-65.

31 Vicencio JM, Lavandero S, Szabadkai G. Ca^{2+}, autophagy and protein degradation: Thrown off balance in neurodegenerative disease. Cell Calcium 2010; 47(2): 112-21.

32 Rasola A, Bernardi P. Mitochondrial permeability transition in Ca^{2+}-dependent apoptosis and necrosis. Cell Calcium 2011; 50(3): 222-33.

The Activity of Inducing Cancer Cell Death and Affecting Mitochondrial Function of a Novel Manganese-pyridine Compound

Zhao Kaidi[1], Gao Jing[1]*, Li Xiang[1], Li Zan[2], Chen Qiuyun[2]

([1]*School of Pharmacy, Jiangsu University, Zhenjiang 212013, China*;
[2]*School of Chemistry and Chemical Engineering, Jiangsu University, Zhenjiang 212013, China*)

Abstract In this study, anticancer activity of the novel manganese-pyridine compound Adpa-Mn(III) ([(Adpa)Mn(μ_2-O)$_2$Mn(Adpa)]$PF_6 \cdot 8H_2O$ (Adpa=bis(2-pyridylmethyl) amino-2-propionic acid)) and its possible mechanism were investigated. Four human cancer cell lines including HepG-2, HeLa, A549 and U251 cells were treated by manganese-pyridine derivative Adpa-Mn(III). Cancer cell proliferation were detected by MTT assay. To observe cell apoptosis, the morphological and nuclei changes in H_2B-GFP-labled HeLa cells were observed by a live cell system (LCS). Autophagic cell death was studied with acidic vesicular organelles observation following monodansylcadervarine (MDC) labeling and autophagy-related proteins GFP-LC3 plasmid transfection. Mitochondrial membrane potential was observed by JC-1 staining; Intracellular free Ca^{2+} content was detected with Fluo-3 staining; Formation of ROS were detected by DCFH-DA staining. Our data show that Adpa-Mn(III) exhibited significant inhibition on cancer cell proliferation and exhibited dose- and time-dependent effect on U251 proliferation. Adpa-Mn(III) induced apoptosis indicated by chromatin condensation. Treartment of Adpa-Mn(III) enhanced fluorescence intensity of monodansylcadervarine (MDC) and GFP-LC3. Moreover, Adpa-Mn(III) induced mitochondrial membrane potential decreased, elevated ROS, and overloaded intracellular Ca^{2+}. These results suggest that Adpa-Mn(III) exerts significant anticancer activity. Adpa-Mn(III) may induce apoptosis and autophagy of cancer cells. The possible mechanism underlying its anticancer effect was related to ROS-induced mitochondrial dysfunction. In summary, the current study suggest that Adpa-Mn(III) could be exploited as a potential lead compound as a novel anticancer metal-drug.

Key words mitochondria; autophagy; apoptosis; ROS; Ca^{2+}

Received: February 28, 2012 Accepted: March 30, 2012

This work was supported by the National Natural Science Foundation of China (No.20971059/B0104), Natural Science Foundation of Jiangsu Province (No.BK2008244) and Society Developing Program of Zhenjiang (No.SH2008072)

*Corresponding author. Tel/Fax: 86-511-88791552, E-mail: jinggao@ujs.edu.cn